Materials Research, Vol. 7, No. 2, 349-354, 2004.

Mathematical Modeling and Experimental Analysis of the Hardened Zone in Laser Treatment of a 1045 AISI Steel

Noé Cheung, Maria Aparecida Pinto, Maria Clara Filippini Ierardi*, Amauri Garcia

Department of Materials Engineering
State University of Campinas - UNICAMP
P.O. Box 6122, 13083-970 Campinas - SP, Brazil

Received: February 14, 2003; Revised: November 7, 2003

The aim of this work is to develop a mathematical model to predict the depth of laser treated zone in the LTH process. The Fourier equation of heat conduction is solved by using the Finite Difference Method in cylindrical coordinates in order to study the temperature distribution produced in a workpiece and hence to obtain the depth to which hardening occurs. The theoretical simulations are compared with results produced experimentally by a CO_2 laser operating in continuous wave, showing good agreement.

Keywords: *mathematical modelling, laser transformation hardening, finite difference method, numerical simulation*

1. Introduction

An increasing number of technological applications requires the operation of mechanical components, such as gears, pistons and bearing, under severe conditions of high stresses located on the workpiece surface. In view of this, effort has been put into the development of surface modification techniques producing new surface materials, with different properties from those of the base. Nowadays, even in traditional realms of classic hardening techniques, such as flame and induction hardening, modern lasers with high quality beams surpassed classic methods with a unique precision and a very intense energy fluxes at the workpiece surface[1-3]. Laser transformation hardening (LTH) is of one the techniques for producing a hard, wear-resistant surface on components, through the action of a scanned laser beam. The LTH process is confined to those materials which exhibit some solid phase transformation and the transformed structures quench to a harder structure than previously. In transformable ferrous alloys, thin surface layers are austenitized and hard martensite is subsequently produced through rapid self-quenching due to the thermal inertia of the substrate material.

As the heating time is short, the hardened zone presents less distortion and surface oxidation than that obtained in flame or induction hardening[4,5]. In addition, the LTH allows the control of the heat treatment process more precisely and introduces automation, leading laser processing an established activity in industry. For the sake of competitiveness in manufacturing, it is necessary to determine the best combination of laser operational parameters for a given application and for a given steel grade. The laser beam parameters such as power density and scan speed exert a great effect on surface layer properties, influencing on transformation into austenite and self quenching leading austenite transformation into martensite[(6)]. The optimization of the LTH process requires the knowledge of other parameters including characteristics of the laser beam, the material properties and particular processing conditions. A multiparameter problem is difficult to solve without extensive factorial experimentation. In addition, when the laser irradiation interacts with a material, the process involved, which occurs on the microscope scale, is very complex making in situ instrumentation a difficult task. Normally, measurement of temperature variation during laser surface treatment is not possible due to the high temperature variation rate. Most of the works in laser surface treatment field analyzes the aftereffects on the

*e-mail: clara1@fem.unicamp.br
Articles presented at the XV CBECIMAT, Natal - RN, November de 2002.

mechanical and chemical properties and on microstrutural transformations. On the other hand, the whole treatment process, mainly during the interaction between laser/material, has much insight in means of mathematical modeling. The simulation of the behavior of complex systems is by now a commonly-adopted procedure when optimizing and controlling industrial processes as a result of the numerical techniques and computer hardware developments. Recent works[7-10] have shown the effectiveness of the use of artificial intelligence coupled with mathematical modeling in order to optimize industrial processes.

There is a good number of published literature[4,11-16] on laser hardening process analyzing thermal and metallurgical effects in the workpiece where phase transformation occurs during the process of heating followed by cooling. Knowledge of the temperature profile provides the prediction of the heat-affected zone, phase composition and hardened layer depth. In order to describe the temperature profile, heat transfer models and mathematical expressions have been developed[17-21].

The aim of this work is to develop a mathematical model to predict the depth of laser treated zone in the LTH process. The phenomenological description of this process is given by the Fourier equation, which describes the way in which the absorbed energy is transmitted throughout the irradiated material. The Fourier equation of heat conduction was solved by using the Finite Difference Method in cylindrical coordinates in order to study the temperature distribution produced in a workpiece and hence obtain the depth to which hardening occurs by analyzing the cooling rates according to the continuous cooling diagram. The theoretical simulations are compared with results produced experimentally by a CO_2 laser operating in continuous wave, showing good agreement.

2. Mathematical Model

To predict theoretically the temperature field of a laser heat treatment, a number of factors should be considered such as: beam intensity profile, the absorption property of the surface to light energy, the boundary conditions of workpiece and the change in the thermal conductivity with temperature.

In this work, the estimation of heat treatment is based on the following assumptions:

- the laser beam is regarded as Gaussian beam of base-mode;
- the treated material is homogeneous;
- thermo-physical properties are dependent on temperature;
- semi-infinite medium.

The time-dependent heat conduction in the space underneath the irradiated surface is described by the Equation[22]:

$$\frac{1}{r}.\frac{\partial}{\partial r}\left(k.r.\frac{\partial T}{\partial r}\right)+\frac{1}{r^2}.\frac{\partial}{\partial \phi}\left(k.\frac{\partial T}{\partial \phi}\right)+\frac{\partial}{\partial z}\left(k.\frac{\partial T}{\partial z}\right)+\dot{q}=\rho.c.\frac{\partial T}{\partial t} \quad (1)$$

where ρ = density (kg/m^3);
c = specific heat (J/kg.K);
k = thermal conductivity (W/m.K);
T = temperature (K);
t = time (s);
r, z = cylindrical coordinates (m);
ϕ = azimuthal angle (rad);
$\dot{q}$ = rate of energy generation (W/m^3).

Figure 1 shows the boundary conditions used to develop the mathematical model.

Equation 1 is reduced to bi-dimension form due to the symmetry according to the ϕ coordinate. The effect of enthalpy of the microestrutural transformation, e.g. austenite-martensite, on the temperature is negligible[23]. In this sense, the rate of energy generation is neglected:

$$k.\left(\frac{\partial^2 T}{\partial r^2}+\frac{1}{r}.\frac{\partial T}{\partial r}\right)+\frac{\partial}{\partial z}\left(k.\frac{\partial T}{\partial z}\right)=\rho.c.\frac{\partial T}{\partial t} \quad (2)$$

In addition, the symmetry condition demands that the heat flow in the (r) direction immediately on the left is equal to the one immediately on the right:

$$q''_{-1,j}=q''_{1,j} \quad (3)$$

where the subscripts $_{-1}$ and $_1$ represent respectively the positions in the (r) direction immediately on the left and on the right of the simmetry axis and the subscript $_j$ represents the positions in the (z) axis.

The workpiece region at $z = \infty$ is considering semi-infinite medium:

$$T(i,\infty,t)=T(\infty,j,t)=T_{env} \quad (4)$$

where i = position in (r) axis;
T_{env} = environment temperature.

At the workpiece outer surface at $z = 0$ part of the energy delivered by laser radiation is absorbed in a thin surface layer of the sample and transferred to the inner part by heat conduction:

$$k.\left.\frac{\partial T}{\partial z}\right|_{i,0}=I'' \quad (5)$$

where I"= absorbed heat flux (W/m^2) by the workpiece surface.

The heat conduction Eq. 2 and the set of boundary conditions are implemented via an explicit finite difference procedure. The terms in the unsteady-state heat conduction equation are replaced by equivalent, although approximate, finite-difference terms which can be obtained from the Taylor series or from a simple heat balance involving adjacent elements, and Eq. 2 can be written as:

$$T_{i,j}^{n+1} = \frac{\Delta t}{\rho_{i,j}.c_{i,j}}.\left[\frac{ke_{i-1,j}.(r_{i,j}-0.5.\Delta r).\left(T_{i-1,j}^{n}-T_{i,j}^{n}\right)+ke_{i+1,j}.(r_{i,j}+0.5.\Delta r).\left(T_{i+1,j}^{n}-T_{i,j}^{n}\right)}{r_{i,j}.\Delta r^{2}}+\ldots\right.$$

$$\left.\ldots+ke_{i,j+1}.\frac{T_{i,j+1}^{n}-T_{i,j}^{n}}{\Delta z^{2}}+ke_{i,j-1}.\frac{T_{i,j-1}^{n}-T_{i,j}^{n}}{\Delta z^{2}}\right]+T_{i,j}^{n} \qquad (6)$$

where T^n and T^{n+1} refer to temperatures before and after the incremental time Δt;
Δz, Δr are the incremental space;
Δt is the incremental time.

ke is the equivalent thermal conductivity in terms of the thermal conductivity of an adjacent element and itself. For example, $k_{eqi+1,j}$ represents the thermal conductivity between the elements (i,j) and (i+1,j) [24]:

$$ke_{i+1,j} = \frac{2.k_{i,j}.k_{i+1,j}}{k_{i,j}+k_{i+1,j}} \qquad (07)$$

The implementation of the presented equations in finite difference form on computer language is aimed to determine the temperature distribution in the heat affected zone and the cooling rate to obtain the harden depth caused by a martensitic transformation.

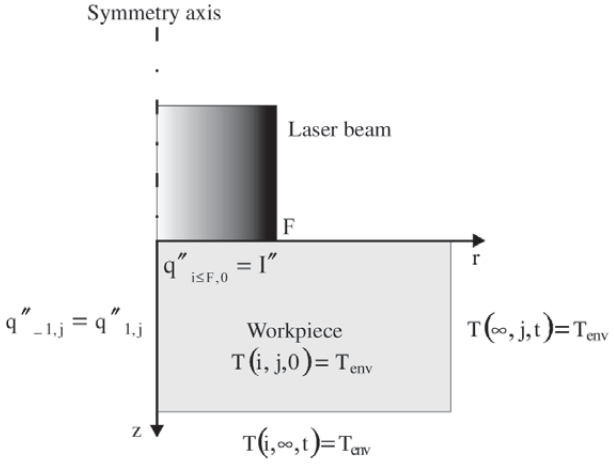

Figure 1. Schematic representation of the boundary conditions.

3. Validation of The Model

A previous validation of the developed mathematical model was achieved by comparing the simulated martensitic delimitation zone with the one generated by the model of Bokota[6] for the case of processing a AISI 1089 steel sample under the action of a laser beam having a Gaussian distribution of energy, power of 1500 W and scanning speed of 16.67 mm/s. It is found a good correlation between the delimited martensitic zones, as shown in Fig. 2. The difference between the results may be attributed to the lack of thermo-physical data which are not furnished in reference (6). The developed model uses the thermo-physical data of AISI 1086 steel from reference (25).

In this study, a CO_2 laser from the Laboratório Nacional de Luz Síncrotron operating in continuous wave was used for surface hardening of a AISI 1045 steel. This type of steel was chosen for the studies because such steels are typical candidate materials for a variety of automobile components that require local hardening. AISI 1045 steel samples were polished by using sand blast in order to ensure uniform finishing. The laser machine operated with a power of 160 W, beam radius of 0.15 mm and scan speeds of 2.67×10^{-1} m/s and 3×10^{-1} m/s. These two speeds produced hardened layers without melting the surface, which is normally undesirable during hardening. Top surface of the laser track scanned at a speed of 2.67×10^{-1} m/s speed is observed where ripples on the surface track are not noticed, indicating that melting does not occur. After the laser surface hardening, samples were prepared for microstructural examination on transverse sections. Microstructural investigations of the transverse section were carried out by using a scanning electron microscope Jeol JSM-5900 and an image processing system Neophot 32 and Leica Q-500 MC.

The CCT diagram of the AISI 1045 steel was obtained

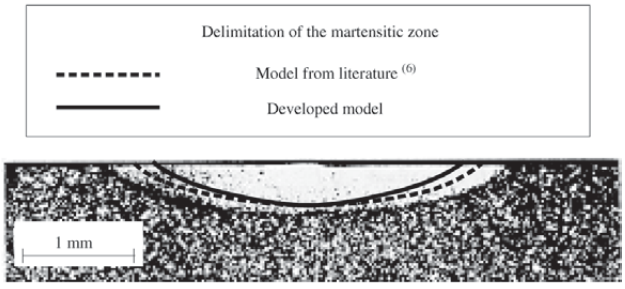

Figure 2. Comparison between the martensitic zone delimitations by the developed model and the one calculated by the Bokota model[6].

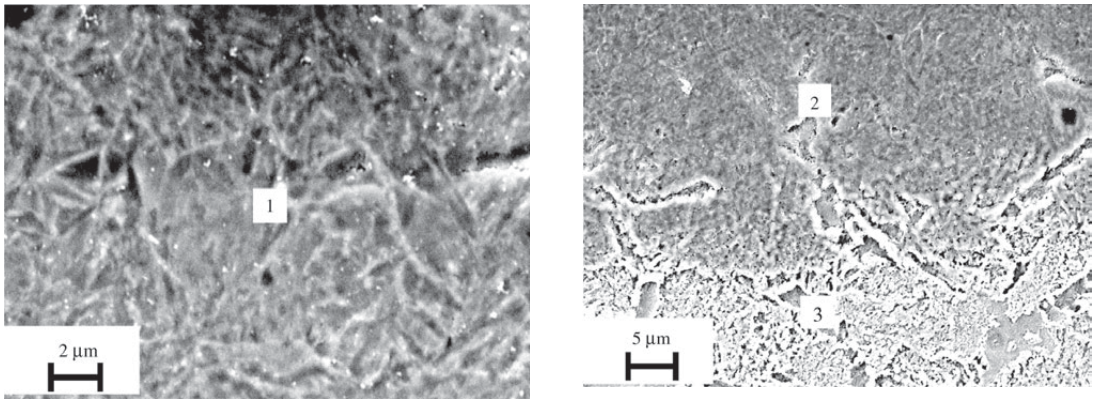

(a)

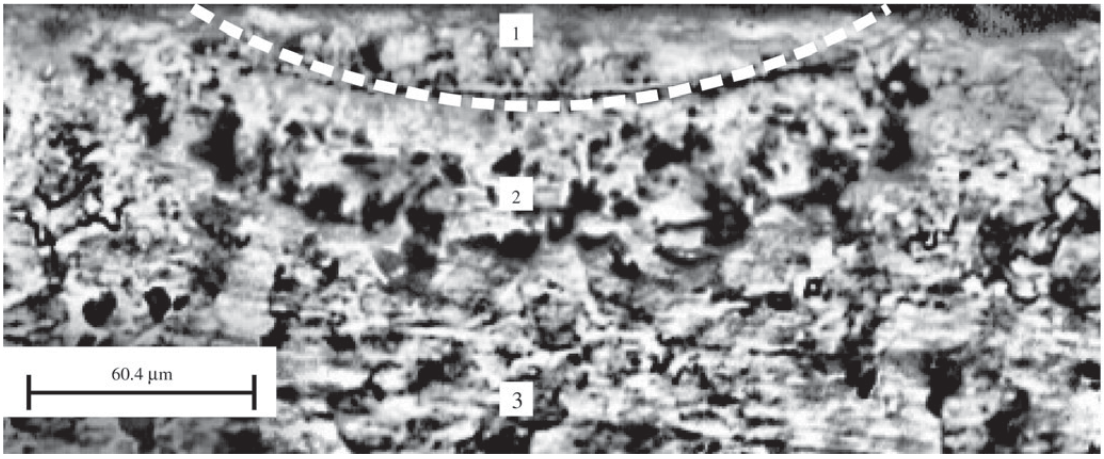

(b)

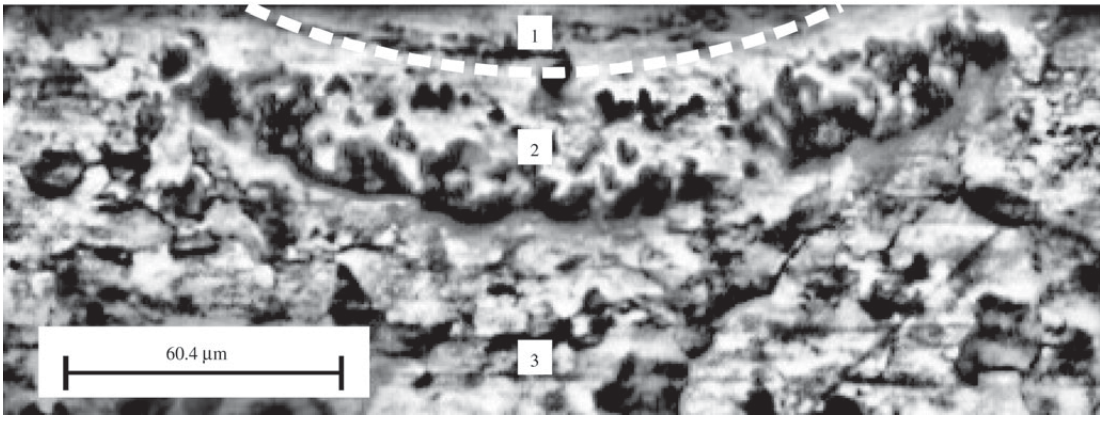

(c)

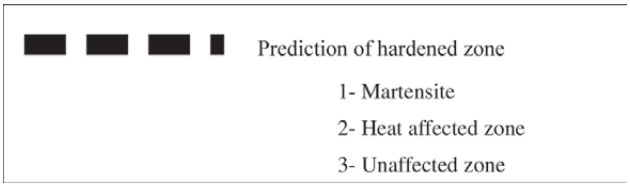

Figure 3. Microstructure of the laser treated zones
a) Magnification of the Zones 1, 2 and 3
b) Martensitic zone prediction by numerical simulation - laser scan speed= 2.67×10^{-1} m/s;
c) Martensitic zone prediction by numerical simulation - laser scan speed= 3×10^{-1} m/s;

from the reference (26) and the corresponding thermal properties (specific heat, thermal conductivity and density) are dependent on temperature and were obtained from reference (27).

The comparison between the simulated and experimental results is shown in the Fig. 3. It can be observed a good agreement between the results. It can also be seen that there is a reduction in the heat affected zone when the beam speed increases from 2.67×10^{-1} m/s to 3×10^{-1} m/s. This fact is due to a smaller dwell time laser/matter, or in other way less energy is delivered to the material surface.

Three different microstructures can be observed in Fig. 3. The unaffected region, a structure equal to the core material, is represented in Zone (3). In Zone (2), the temperature is above the eutectoid but below the austenisation temperature. Perlite colonies transformed into austenite, which upon subsequent cooling transformed into martensite. Due to the high heating rate, these perlite colonies did not have sufficient time to interact with their neighboring ferrite. In zone (1), maximum temperatures are located and since diffusion coefficient is strongly influenced by temperature, homogenization of carbon concentration is achieved. Vickers microhardness tests were carried out in the three zones. The test load for all zones was set up by 20 gf in the Neophot 32 microhardness testing system. The average hardness increases from 258 HV in the unaffected zone to 768 HV in the heat affected zone (HAZ), which indicates that in HAZ there is a mixture of martensite and ferrite. In contrast, a higher value of 1021 HV is achieved in the zone (3) due to the martensitic structure.

4. Conclusions

A numerical model of a transient two-dimensional laser hardening process based on the finite difference method in cylindrical coordinates was developed. It is shown that the numerical predictions of the hardened layer are in good agreement with the experimental results, which permits to conclude that the mathematical model is a useful tool to predict the depth during laser hardening. Mechanical Vickers hardness measurements have been carried out along the treated cross sections, and it was found that values of about four times higher than those observed in the original substrate can be attained, confirming the effectiveness of the laser treatment.

Acknowledgements

The authors acknowledge the financial support provided by FAPESP (The Scientific Research Foundation of the State of São Paulo) and CNPq (The Brazilian Research Council). The authors also thank Laboratório Nacional de Luz Sincrotron for technical support during electron microscopy work and Mr. Eli Siqueira Wenzel for processing the samples in a laser machine.

References

1. Damborenea, J. *Surface Coat Tech,* v. 100-101, p. 377-382, 1998.
2. Ion, J.C.; Shercliff, H.R.; Ashby, M.F. *Acta Metall Mater*, v. 40, p. 1539-1551, 1992.
3. Monson, P.J.E.; Steen, W.M. *Surface Eng,* v. 6, p. 185-193, 1990.
4. Ashby, M.F.; Easterling, K.E. *Acta Metall Mater,* v. 32, p. 1935-1948, 1984.
5. Woo, H.G.; Cho, H.S. *Surface Coat Tech,* v. 102, p. 205-217, 1998.
6. Bokota, A.; Iskierka, S. *Acta Mater,* v. 44, p. 445-450, 1996.
7. Kumar, S.; Meech, J.A.; Samarasekera, I.V. *Brimacombe, J. K I&SM,* p. 29-36, 1993.
8. Filipic, B.; *Sarler, B. Proceedings os the 6th European Congress on Intelligent Techniques and Soft Computing, Aachen, Germany* 1998.
9. Cheung, N.; Ierardi, M. C. F.; Garcia, A.; *Vilar, R. Lasers Eng, v.* 10, p. 275-291, 2000.
10. Cheung, N.; Garcia *A. Engineering Applications of Artificial Intelligence,* v. 14, p. 229-238, 2001.
11. Merling, J.; Renard, C.; *Bignonnet, A Li Junchang, Matériaux et Techniques Été,* v. 92, p. 6-8, 1992.
12. Putatunda, S.K.; Nambiar, M.; *Clark, N Surface Eng,* v. 13, p. 407-414, 1997.
13. Shiue, R.K.; *Chen, C. Scripta Metall Mater,* v. 25, p. 1889-1894, 1991.
14. Shiue, R.K.; Chen, C. *Metall Trans A,* v. 23, p. 163-170, 1992.
15. Yang, L.J.; Jana, S.; Tam, S.C. *J. Mater Process Tech,* v. 23, p. 133-147, 1990.
16. Yang, L.J.; Jana, S.; Tam, S.C.; *L. E. N. Lim, Mater Manuf Process,* v. 9, p. 475-492, 1994.
17. Reti, T.; Bagyinszki, G.; Felde, I.; Verö, B.; Bell, T. *Comp Mater Sci,* v. 15, p. 101-112, 1999.
18. Ruiz, J.; Fernández, B.J.; Ma, J.; *Belló, Key Eng Mat,* v. 46-47, p. 161-174, 1990.
19. Shang, H.M. *J Mater Process Tech,* v. 23, p. 65-72, 1990.
20. Davis, M.; Kapadia, P.; Dowden, J.; Steen, W.M.; Courtney, C.H.G. *J Appl Phys Dc,* v. 19, p. 1981-1996, 1986.
21. Zubair, S.M.; Aslam Chaudhry, M. *Int J Heat and Mass Transfer,* v. 39, p. 3067-3074, 1996.
22. Incropera, F.P.; Dewitt, D.P. *Fundamentals of Heat and Mass Transfer, John Wiley & Sons, New York,*1990.
23. Jansson, B.; Rolfson, M.; Thuvander, A.; Melander, A.; Wullimann, C. *Materials Science and Technology,* v. 7, p. 118-127, 1991.

24. Ruddle, R. W. *The solidification of castings, Institute of Metals, Series No. 7,* 1957.
25. Pehlke, R.D. *et al. Summary of thermal properties for casting alloys and mold materials, University of Michigan,* 1982.
26. Atkins, M. *Atlas of continuous cooling transformation diagrams for engineering steels, British Steel Corp., ASM, Metals Park,* 1980.
27. Dardel, Y. *Edition de la Revue de Metalurgie,* p. 211-226, 1964.